ISSN 0005-1144
ATKAFF 51(2), 174–180(2010)

David Stojan, Miro Milanovič

Over-modulation phenomena and its influence on the pulse width modulated single-phase inverter output voltage

UDK 621.376.5
IFAC 5.8.6

Original scientific paper

This paper describes analysis of the pulse width modulated single-phase inverter output voltage. By using the over-modulation principle the low THD distortion of the output voltage appears but the first voltage harmonic is increased. The root mean square (RMS) component of the output voltage is also increased. Due to this phenomenon the dc converter input voltage can be decreased, which is always welcomed.

Key words: Over-modulation, single-phase voltage inverter, THD

Premodulacija i njezin utjecaj na izlazni napon jednofaznog izmjenjivača s modulacijom širine impulsa. U članku je analizirana modulacija širine impulsa kod jednofaznog izmjenjivača. Amplituda osnovnog harmonika napona može se povećati modulacijskim indeksom većim od 1. U tom se slučaju povećava ukupna harmonijska distorzija, koju je moguće držati u zadanim granicama. Pri tome se povećava efektivna vrijednost izmjenične komponente izlaznog napona izmjenjivača. Korištenjem premodulacije moguće je sniziti ulazni napon pretvarača, što se uglavnom i preporučuje.

Ključne riječi: premodulacija, jednofazni izmjenjivač, ukupna harmonijska distorzija

1 INTRODUCTION

Single-phase inverters are used in battery powered systems (uninterruptible power system - UPS) and in active power factor correction single-phase AC rectifiers. In such circuits MOS-FETs and IGBTs have usually been used, depending on the presumed requirements.

The control and modulation of single-phase inverters have been studied in many references such as [1–5]. In [6] the author describes a survey of pulse width modulation techniques appropriate for single and three-phase systems. The well-known phenomena in inverter circuits due to dead-time introduction, in order to avoid short cuts according to input inverter terminals are described in [2]. Authors described an effective approach to compensate for this necessary but undesirable phenomenon. The appropriate PWM is always used in all these applications. The over-modulation phenomenon is widely used in three-phase systems in order to extend the output voltage range by introducing third voltage harmonics in the modulation procedure.

This paper deals with an analytical evaluation of the over-modulation phenomena in single-phase inverters circuits, where the main goal was to decrease the input DC voltage while keeping the RMS value and THD factor of output voltage at the same level and under prescribed limits. Full-bridge configuration [1] of a single-phase inverter is shown in Fig. 1. The input DC voltage U_d level is considered when switching elements (transistors) are selected in inverter design procedure. Consequently, the price of the inverter semiconductor switches is close connected with the U_d voltage level, therefore if voltage U_d is reduced, then the price of the whole inverter can be reduced and

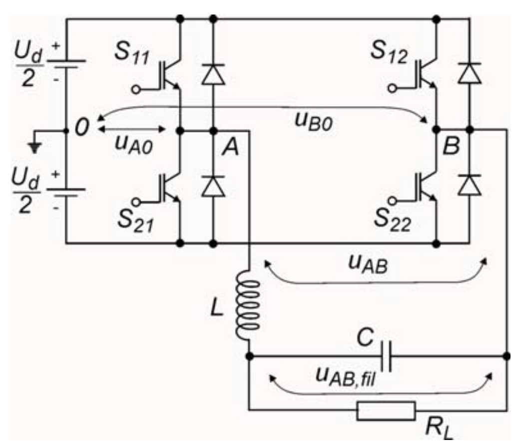

Fig. 1. Schematic of single-phase inverter

at the same time the size and efficiency can be improved. Analytical evaluation of over-modulation phenomena was verified using simulation with MATLAB-Simulink software package, and experimentally.

2 MATHEMATICAL ANALYSIS OF ORDINARY AND OVER-MODULATION REGION

For each inverter leg PWM modulator is needed. In a PWM modulator a desired reference signal is compared with a triangular waveform as shown in Fig. 2. Outcome of the switching scheme shown on Fig. 2 is three-level voltage u_{AB} on the inverter output terminals.

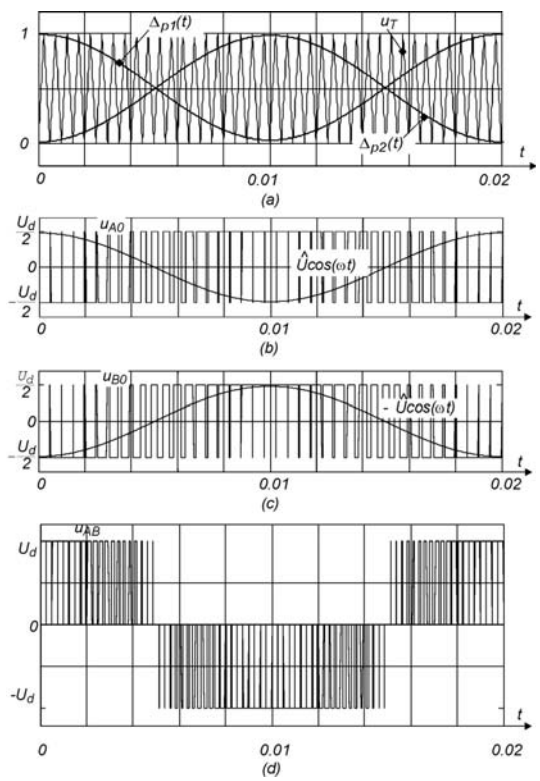

Fig. 2. (a) Switching functions (duty cycle functions), (b) "Single"-phase voltage u_{A0}, (c) "Single"-phase voltage u_{B0}, (c) Three-level voltage u_{AB}

2.1 Ordinary modulation region

In order to generate three-level output voltage u_{AB} the desired reference signal can be calculated by defining the converter output voltage u_{A0} and u_{B0} as a linear combination of the two events [3, 5]:

$$u_{A0} = H_{11}\frac{U_d}{2} + H_{21}\left(-\frac{U_d}{2}\right) = (2H_{11}-1)\frac{U_d}{2}, \quad (1)$$

where U_d represents the converter input voltage and the switching function H_{11} is defined as

$$H_{11} = \begin{cases} 1, \text{ when } S_{11} \text{ is ON, } S_{21} \text{ is OFF} \\ 0, \text{ when } S_{11} \text{ is OFF, } S_{21} \text{ is ON} \end{cases}$$

Moreover, condition $H_{11} + H_{21} = 1$ must be fulfilled to avoid short-circuit in first converter leg. The same procedure follows for voltage u_{B0} evaluation:

$$u_{B0} = H_{12}\frac{U_d}{2} + H_{22}\left(-\frac{U_d}{2}\right) = (2H_{12}-1)\frac{U_d}{2}, \quad (2)$$

where the switching function H_{12} is defined as

$$H_{12} = \begin{cases} 1, \text{ when } S_{12} \text{ is ON, } S_{22} \text{ is OFF} \\ 0, \text{ when } S_{12} \text{ is OFF, } S_{22} \text{ is ON} \end{cases}$$

and likewise condition $H_{12} + H_{22} = 1$ must be fulfilled in order to avoid short-circuit in second converter leg. Hence, voltage u_{AB} is evaluated as follows:

$$u_{AB} = u_{A0} - u_{B0} = (H_{11} - H_{12})\,U_d = (\Delta_{p1} - \Delta_{p2})\,U_d. \quad (3)$$

In (3) switching functions H_{12} and H_{22} are replaced by duty cycle functions Δ_{p1} and Δ_{p2}, respectively (Fig. 3). The duty cycle functions can be computed from (1) and (2). In order to organize the three-level output voltage u_{AB} voltages u_{A0} and u_{B0} must be defined as:

$$\begin{aligned} u_{A0} &= \hat{U}\sin(\omega t), \\ u_{B0} &= -\hat{U}\sin(\omega t), \end{aligned} \quad (4)$$

such that from (1) and (2) the following is obtained:

$$\begin{aligned} \Delta_{p1}(t) &= \tfrac{t_{on1}}{T_s} = \tfrac{1}{2} + \tfrac{1}{U_d}u_{A0} = \tfrac{1}{2} + m_{iA}(t), \\ \Delta_{p2}(t) &= \tfrac{t_{on2}}{T_s} = \tfrac{1}{2} + \tfrac{1}{U_d}u_{B0} = \tfrac{1}{2} + m_{iB}(t), \end{aligned} \quad (5)$$

where $m_{iA}(t)$ and $m_{iB}(t)$ represent the reference signal or reference voltage which is sometimes also called the modulation function. Duty cycle functions in (5) also represent

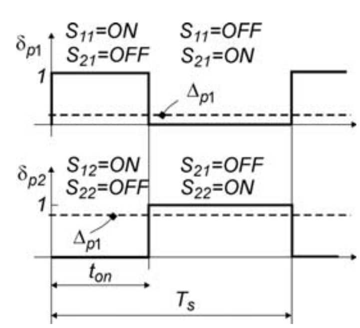

Fig. 3. Switching functions and duty cycle functions

the average switching function value during the interval T_s as shown in Fig. 3. After using (4) in (5) reference voltages can be expressed as:

$$\begin{aligned} m_{iA} &= \frac{\hat{U}}{U_d}\cos(\omega t) = m_I \cos(\omega t), \\ m_{iB} &= -\frac{\hat{U}}{U_d}\cos(\omega t) = -m_I \cos(\omega t), \end{aligned} \tag{6}$$

where $m_I = \hat{U} \big/ U_d$ and represents the modulation index. By comparing the average duty cycle functions (Δ_{p1} and Δ_{p2}, Fig. 2 (a)) with the triangular signal (u_T, Fig. 2 (a)) the PWM signal can be generated and applied to the switches (Fig. 3). The PWM signals are generated as follows:

$$\begin{aligned} \delta_{p1}(t) &= \begin{cases} 1, \text{ when } H_{11} \geq u_T \text{ then } S_{11} \text{ is ON, } S_{21} \text{ is OFF} \\ 0, \text{ when } H_{11} \leq u_T \text{ then } S_{11} \text{ is OFF, } S_{21} \text{ is ON}, \end{cases} \\ \delta_{p2}(t) &= \begin{cases} 1, \text{ when } H_{21} \geq u_T \text{ then } S_{21} \text{ is ON, } S_{22} \text{ is OFF} \\ 0, \text{ when } H_{22} \leq u_T \text{ then } S_{21} \text{ is OFF, } S_{22} \text{ is ON}. \end{cases} \end{aligned} \tag{7}$$

When the instantaneous signals (7) of duty cycle functions $\delta_{p1}(t)$ and $\delta_{p2}(t)$ are applied at the switches (Fig. 4), the voltage u_{AB} is generated at the converter output terminals. Voltage u_{AB} is described as:

$$u_{AB} = (\delta_{p1}(t) - \delta_{p2}(t))\, U_d \tag{8}$$

The PWM functions from (7) are depicted in Fig. 3. Both PWM functions $\delta_{p1}(t)$ and $\delta_{p2}(t)$ (7) can be approximated by using Fourier series [7]:

$$\begin{aligned} \delta_{p1}(t) &= \Delta_{p1}(t) + \textstyle\sum_{n=1}^{\infty} \frac{2}{\pi} \frac{\sin(n\pi\Delta_{p1}(t))}{n} \cos(n\omega_T t), \\ \delta_{p2}(t) &= \Delta_{p2}(t) + \textstyle\sum_{n=1}^{\infty} \frac{2}{\pi} \frac{\sin(n\pi\Delta_{p2}(t))}{n} \cos(n\omega_T t). \end{aligned} \tag{9}$$

After some manipulation by (5), (6) and (9) and after the substitution of (9) into (8) the voltage can be described as follows:

$$\begin{aligned} &u_{AB}(t) = U_d m_I \cos(\omega t) + \tfrac{4U_d}{\pi} \cdot \\ &\cdot \sum_{n=1}^{\infty} \tfrac{1}{n} \cos\left(\tfrac{n\pi}{2}\right) \sin\left(\tfrac{n\pi}{2} + \tfrac{n\pi}{2} m_I \cos(\omega t)\right) \cos(n\omega_T t). \end{aligned} \tag{10}$$

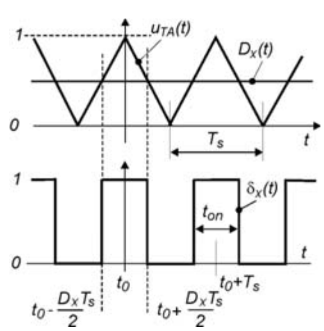

Fig. 4. Triangle waveform (u_{TA}) and generation of the pulse train δ_x

Again, after some manipulation and by using the power of the Bessel series [4] (10) can be written as:

$$\begin{aligned} &u_{AB} = U_d m_I \cos(\omega t) + \tfrac{4U_d}{\pi} \cdot \\ &\cdot \textstyle\sum_{n=1}^{\infty} \frac{1}{n} \left(\cos\left(\frac{n\pi}{2}\right) J_1\left(\frac{n\pi m_I}{2}\right) (\cos((n\omega_T + \omega)t) + \right. \\ &+ \cos((n\omega_T - \omega)t)) - \\ &- \cos\left(\tfrac{n\pi}{2}\right) J_3\left(\tfrac{n\pi m_I}{2}\right) (\cos((n\omega_T + 3\omega)t)) + \\ &+ \cos((n\omega_T - 3\omega)t)) + \\ &+ \cos\left(\tfrac{n\pi}{2}\right) J_5\left(\tfrac{n\pi m_I}{2}\right) (\cos((n\omega_T + 5\omega)t). \end{aligned} \tag{11}$$

Equation (11) was used in order to evaluate the voltage spectrum. The following modulation parameters have been used in order to calculate the voltage spectrum lines: DC voltage $U_d = 350$ V, frequency of synthesized signal $f = 50$ Hz ($\omega = 2\pi f$), $f_T = 2$ kHz ($\omega_T = 2\pi f_T$), and the modulation index $m_I = 1$. The dispositions of the spectral lines are evident from Tab. 1 and Tab. 2, and are depicted in Fig. 5. This shows that the frequency modulated signal $u_{AB}(t)$ has a fundamental component appearing at the frequency ω with a magnitude of $U_d m_I$ and, besides the carrier frequency $2nf_T$, also contains the frequencies $2nf_T \pm kf$, n=1,2,3,...∞, k=±1,±2,..∞. It

Table 1. Spectral lines around the second multiplier of carrier frequency ($2f_T$)

a_{21}	$+\frac{4U_d}{\pi}\frac{1}{2}\cos\left(\frac{2\pi}{2}\right) J_1\left(\frac{2\pi m_I}{2}\right)$	-61.41
a_{23}	$-\frac{4U_d}{\pi}\frac{1}{2}\cos\left(\frac{2\pi}{2}\right) J_3\left(\frac{2\pi m_I}{2}\right)$	-74.3
a_{25}	$-\frac{4U_d}{\pi}\frac{1}{2}\cos\left(\frac{2\pi}{2}\right) J_5\left(\frac{2\pi m_I}{2}\right)$	-11.61

Table 2. Spectral lines around the fourth multiplier of carrier frequency ($4f_T$)

a_{41}	$\frac{4U_d}{\pi}\frac{1}{4}\cos\left(\frac{4\pi}{2}\right) J_1\left(\frac{4\pi m_I}{2}\right)$	-23.66
a_{43}	$-\frac{4U_d}{\pi}\frac{1}{4}\cos\left(\frac{4\pi}{2}\right) J_3\left(\frac{4\pi m_I}{2}\right)$	3.24
a_{45}	$+\frac{4U_d}{\pi}\frac{1}{4}\cos\left(\frac{4\pi}{2}\right) J_5\left(\frac{4\pi m_I}{2}\right)$	-41.53

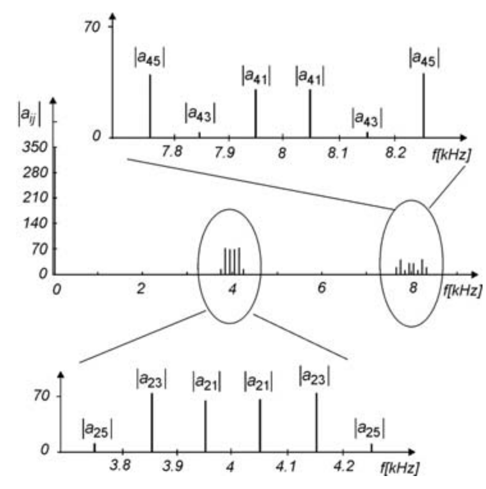

Fig. 5. Calculated spectrum of voltage u_{AB}

is also evident that the spectral line with multiplier of 3 ($k = 3, 6, 9, \dots$), which belongs to the Bessel function $J_3(x)$ disappears from the voltage spectrum.

Such spectrum analysis can be done by using MATLAB (fft analysis) but has no benefit for a deeper understanding of the modulation phenomena. The magnitude of fundamental-frequency voltage varies linearly with m_I when $m_I \leq 1$. When m_I is increased over 1.0 the amplitude of fundamental voltage component does not vary linearly with m_I any more. This phenomenon is called over-modulation.

2.2 Over-modulation region

"Single-phase" voltage $u_{A0}(t)$ in the over-modulation region is shown Fig. 6. Both voltages $u_{A0}(t)$ and $u_{B0}(t)$ can be described by:

$$u_{A0}(t) = \begin{cases} U_d/2; & 0 \leq \omega t \leq \alpha, \\ \hat{U}\cos(\omega t); & \alpha \leq \omega t \leq \pi - \alpha, \\ -U_d/2; & \pi - \alpha \leq \omega t \leq \pi + \alpha, \\ \hat{U}\cos(\omega t); & \pi + \alpha \leq \omega t \leq 2\pi - \alpha, \\ U_d/2; & 2\pi - \alpha \leq \omega t \leq 2\pi \end{cases} \tag{12}$$

$$u_{B0}(t) = \begin{cases} -U_d/2; & 0 \leq \omega t \leq \alpha, \\ -\hat{U}\cos(\omega t); & \alpha \leq \omega t \leq \pi - \alpha, \\ U_d/2; & \pi - \alpha \leq \omega t \leq \pi + \alpha, \\ -\hat{U}\cos(\omega t); & \pi + \alpha \leq \omega t \leq 2\pi - \alpha, \\ -U_d/2; & 2\pi - \alpha \leq \omega t \leq 2\pi, \end{cases} \tag{13}$$

where α is indicated in Fig. 6 and can be calculated as follows:

$$\alpha = \arccos\left(\frac{U_d}{2\hat{U}}\right). \tag{14}$$

According to (5) the duty cycle function can now be represented slightly different:

$$\begin{aligned} \Delta_{p1}(t) &= \tfrac{1}{2} + \tfrac{1}{U_d} u_{A0}, \\ \Delta_{p2}(t) &= \tfrac{1}{2} + \tfrac{1}{U_d} u_{B0}, \end{aligned} \tag{15}$$

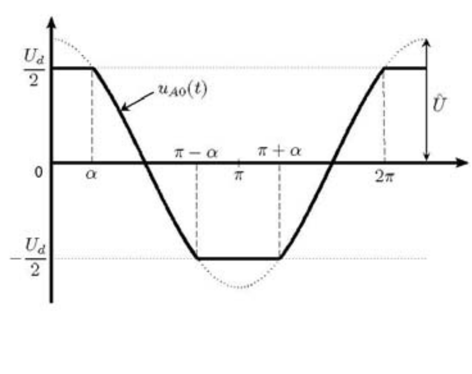

Fig. 6. "Single" phase voltage $u_{A0}(t)$

where u_{A0} and u_{B0} must be considered as follows from (13). So the duty cycle functions are now described by expanding u_{A0} and u_{B0} using the Fourier series. It yields:

$$\begin{aligned} \Delta_{p1}(t) &= \tfrac{1}{2} + \tfrac{1}{U_d}\left(b_1 \sin x + b_3 \sin 3x + b_5 \sin 5x + \cdots\right), \\ \Delta_{p2}(t) &= \tfrac{1}{2} - \tfrac{1}{U_d}\left(b_1 \sin x + b_3 \sin 3x + b_5 \sin 5x + \cdots\right), \end{aligned} \tag{16}$$

where coefficients $b_1, b_3, b_5 \dots$ are calculated by using formulas

$$\begin{aligned} a_n &= \tfrac{2}{T}\int_0^{T/2} [f(\omega t) + f(-\omega t)]\cos(n\omega t)dt, \\ b_n &= \tfrac{2}{T}\int_0^{T/2} [f(\omega t) - f(-\omega t)]\sin(n\omega t)dt. \end{aligned}$$

After some mathematical operations, the general term for the arbitrary harmonic component is described by:

$$\begin{aligned} b_n \;=\; & \tfrac{2U_d}{\pi}\Big[\tfrac{1}{(n-1)} m_I \sin((n-1)\alpha) \\ & + \tfrac{1}{n}\cos(n\alpha) - \tfrac{1}{(n+1)} m_I \sin((n+1)\alpha)\Big]. \end{aligned} \tag{17}$$

These particular coefficients can be calculated from (17) as follows:

$$\begin{aligned} b_1 &= \tfrac{2U_d}{\pi}\left[m_I\alpha + \tfrac{1}{1}\cos 1\alpha - \tfrac{1}{2} m_I \sin 2\alpha\right], \\ b_3 &= \tfrac{2U_d}{\pi}\left[\tfrac{1}{2} m_I \sin(2\alpha) + \tfrac{1}{3}\cos(3\alpha) - \tfrac{1}{4} m_I \sin(4\alpha)\right], \\ b_5 &= \tfrac{2U_d}{\pi}\left[\tfrac{1}{4} m_I \sin(4\alpha) + \tfrac{1}{5}\cos(5\alpha) - \tfrac{1}{6} m_I \sin(6\alpha)\right], \\ &\vdots \end{aligned} \tag{18}$$

Figure 7 shows the first voltage harmonic magnitude. It is evident that the first harmonic can be increased over the value U_d. In order to evaluate the appropriate increase of the first harmonic in the over-modulation area, it is necessary to also calculate the total harmonic distortion factor (THD). According to the definition, THD can be evaluated as follows:

$$THD = \sqrt{\frac{\sum_{h=2}^{\infty} \hat{U}_h^2}{\hat{U}_1^2}}. \tag{19}$$

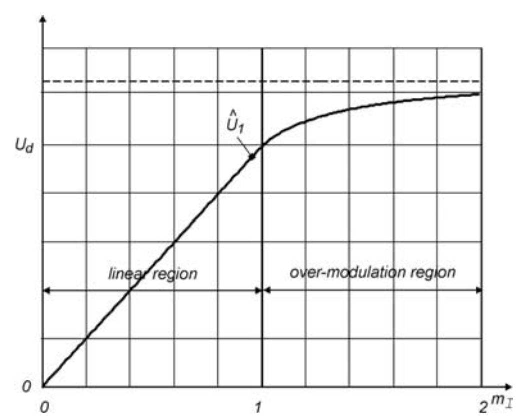

Fig. 7. Fundamental-frequency voltage $\hat{U}_1 = f(m_I)$

Thus by using the series as follows from (17) and (18), the particular harmonics and THD can be evaluated, as shown in Fig. 8. When a specific THD is chosen (usually this is load requirement) it is evident from the analysis and also from the THD calculation as to how the first voltage harmonic can be increased in order to keep the THD under the prescribed value. For example, when a THD of 10% has been chosen, the first harmonics can be increased app. for 16%. From this fact, it follows that the DC voltage can also be decreased. For example, in order to have 230 V RMS at the converter output in the case of ordinary modulation ($m_I = 1.0$) $U_d = 324$ V must be chosen, but by using the over-modulation region ($m_I = 1.4$), the DC voltage can be decreased to $U_d = 280$ V. The over-modulation phenomena is always welcome in cases where DC voltage U_d is produced from voltage sources as for solar panels or fuel cell systems, and need to be boosted by using the DC-DC boost converter.

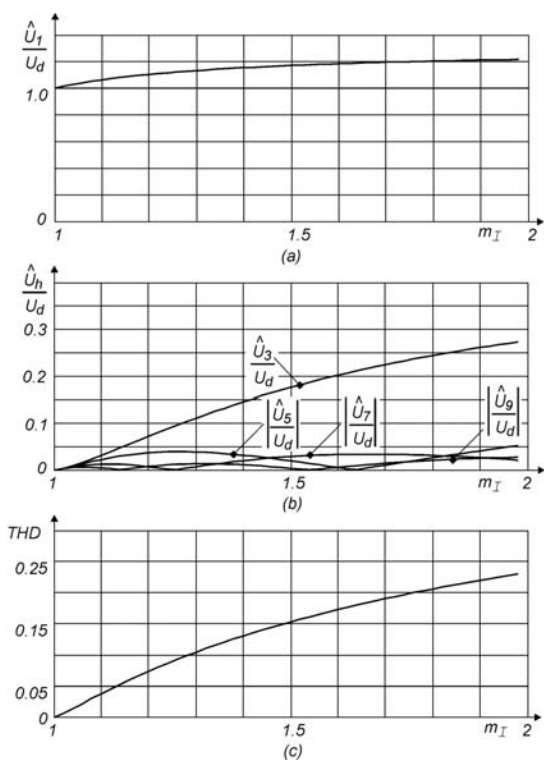

Fig. 8. (a) The first harmonic voltage component in the over-modulation region; (b) The higher harmonics voltage components in the over-modulation region; (c) THD in the over-modulation region

3 SIMULATION

The harmonic analyzing method, analytical results and their consequences were verified by simulation. Simulations were done with input voltage $U_d = 325$ V and ideal transistors were chosen. The dead-time effect was neglected. Considering (18) by choosing $m_I = 1.133$ the first harmonic component can be increases by 8% and at $m_I = 1.285$ by 13%.

Using expression $U_d = 230 \cdot \sqrt{2}/1.08$ the voltage U_d can be reduced to 301 V at $m_I = 1.133$ and to 290 V at $m_I = 1.285$. According to the scheme in Fig. 9, the bandwidth of output filter was set at 10 kHz ($L = 250$ μH and $C = 1$ μF), with $R_L = 100$ Ω of load, the switching frequency was set to 50 kHz. Figure 10 and Fig. 11 show simulation results. It can be seen that input voltage can be decreased. Figure 11 shows filtered and non-filtered unipolar output voltage at modulation ratio $m_I = 1.285$. The voltage u_{AB} was filtered so that over-modulation is visible.

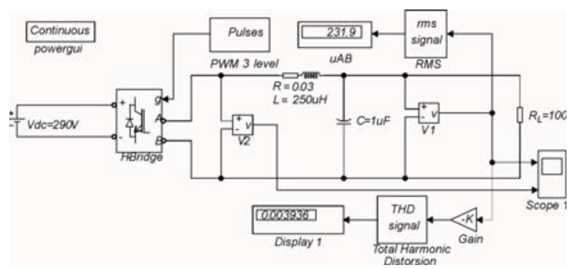

Fig. 9. Simulation scheme of a single-phase inverter

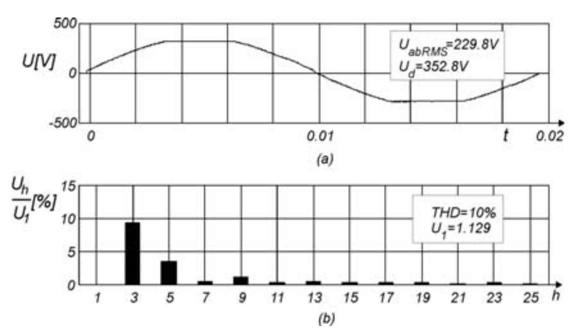

Fig. 10. Simulation results for $m_I = 1.133$, $U_d = 301$ V

4 EXPERIMENTAL RESULTS

To verify analytical and simulation results the preprogrammed PWM inverter was implemented with a dsPIC digital signal processor. The experiments were carried out

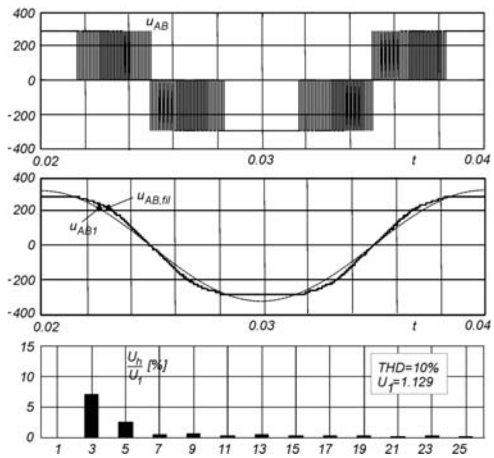

Fig. 11. Simulation results; filtered and non-filtered output voltage for $m_I = 1.285$*,* $U_d = 290$ V

within the following filter circuit parameters:

$$L = 250\ \mu\text{H},$$
$$C = 2.2\ \mu\text{F},$$
$$P_{\text{load}} = 1\ \text{kW}.$$

Fig. 12 shows measured results for the first experiment when a DC voltage of $U_d = 330$ V was applied. A modulation index of $m_I = 0.98$ was chosen in order to establish the 230 V RMS. Due to dead-time effect, which has been introduced into the modulation algorithm in order to avoid short-circuits in both of the converter's legs, total harmonic distortion was 2.3%.

Figure 13 shows second experiment, when over-modulation algorithm was applied. The modulation index was 1.285 and THD was limited to 10%. In order to establish 230 V RMS on the output, the input DC voltage can

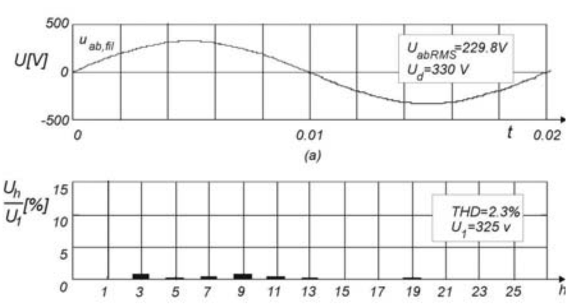

Fig. 12. Sine wave output voltage and odd harmonics $m_I = 0.98$

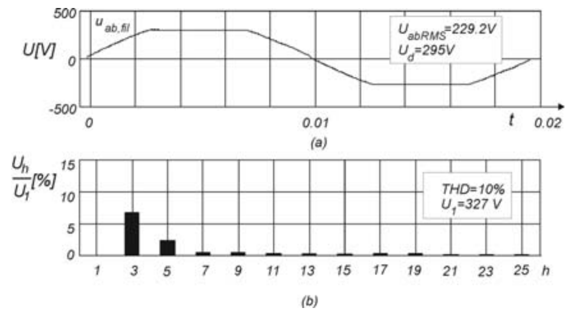

Fig. 13. Over-modulated sine wave output voltage and odd harmonics $m_I = 1.285$

be decreased to $U_d = 295$ V. These results were in accordance with the theoretical and simulation predicted results.

5 CONCLUSION

This paper describes over-modulation phenomena in a single-phase inverter. It has been shown that the mathematical and physical connections among modulation parameters (modulation index, desired THD) have an influence to the desired input and output voltages. It has also been shown that inverter input voltage can be reduced due to use of over-modulation, which is appropriate when low-voltage sources with a booster are applied during the power conversion process (solar panels, fuel cells...). The analytical approach to a modulation algorithm enables further investigation in the direction of harmonic minimization of components within the voltage spectra.

REFERENCES

[1] M. Milanovič, *Močnostna elektronika*. FERI Maribor, 2007.

[2] N. Mohan, T. Undeland, and W. Robbins, *Power Electronics Converters: Applications and Design*. John Wiley & Sons, Inc., 1995.

[3] P. Krein, *Elements of Power Electronics*. Oxford: University Press, 1998.

[4] R. Ericson and D. Maksimovic, *Fundamentals of Power electronics*. Kluwer Academic Publisher, 2001.

[5] P. Wood, *Switching Power Converters*. New York: ??, 1981.

[6] H. Van der Broeck, "Analysis and realization of pulse width modulator based on voltage space vectors," in *Proceedings of the 1986 IEEE-IAS Annual Meeting*, pp. 244–251, 1986.

[7] N. Bronstein, K. Semndljajew, G. Musiol, and H. Muhlig, *Matematični priročnik*. Tehniška založba Slovenije, 1997.

David Stojan received the B.Sc. degree in electrical engineering from the University of Maribor, Maribor, Slovenia in 2005. From 2005 to 2008 he worked as engineer for maintenance of distribution substations at power distribution company Elektro Celje d.d. in Celje, Slovenia. From 2008 to the present he works as young researcher at Research and Development centre of Electrical Machines (TECES) in Maribor, Slovenia. His main research interests are motor control, control algorithms and power electronics.

Miro Milanovič received the B.Sc., M.Sc. and the doctorate degrees in electrical engineering from the University of Maribor, Maribor, Slovenia in 1978, 1984, and 1987, respectively. From 1978 to 1981 he worked as a Power Electronics Research Engineer at TSN Co. Maribor, Slovenia. From 1981 to the present he has been a Faculty member of the Faculty of Electrical Engineering and Computer Sciences, University of Maribor, Slovenia. In 1993 he was a visiting scholar at the University of Wisconsin, Madison, USA and in 1999 he spent two months at the University of Tarragona, Spain as a Visiting Professor. Currently he has a full professor position at the University of Maribor and he also holds a head position at Institute of robotics. His main research interests include control of power electronics circuits, unity power factor correction and switching matrix converters. He has published a great number of papers in scientific journals and conference proceedings. He has authored three books in Slovenian language, "Analogna integrirana vezja v industrijski elektroniki" (Analog Integrated Circuits in Industrial Electronics), "Uvod v močnostno elektroniko" (Introduction to Power Electronics), and "Močnostna elektronika" (Power Electronics).

AUTHORS' ADDRESSES
David Stojan[1],
Prof. dr. Miro Milanovič[1,2],
[1]TECES, Podbreška cesta 20,
2000 Maribor, Slovenia
[1,2] University of Maribor,
Faculty of Electrical Engineering and Computer Sciences,
Smetanova 17, 2000 Maribor, Slovenia
email: david.stojan@teces.si, milanovic@uni-mb.si

Received: 2009-06-17
Accepted: 2009-12-03